6-2013

# Development and Validation of a Computational Model for Studying Secondary Droplet Breakup in Time-Varying Flows

Brandan A. West
*Union College - Schenectady, NY*

# Development and Validation of a Computational Model for Studying Secondary Droplet Breakup in Time-Varying Flows

By

Brendan Adams West

* * * * * * * * *

Submitted in partial fulfillment

of the requirements for

Honors in the Department of Mechanical Engineering

UNION COLLEGE

June, 2013

ABSTRACT

WEST, BRENDAN Development and Validation of a Computational Model for Studying Secondary Droplet Breakup in Time-Varying Flows. Department of Mechanical Engineering, June 2013.

ADVISOR: Bradford Bruno

Secondary droplet breakup is an important topic in fluid mechanics that has applications in many atomization processes. To date, the experimental and computational research of secondary droplet breakup has focused primarily on the breakup process in flows that have steady velocities. This study utilizes computational fluid dynamics software called Star-CCM+ Version 7.04.006 to study the effects of time-varying flows on the droplet breakup process. Time-varying flows are more representative than steady flows are of the flow situations in combustion chambers of high-level engines such as jet and rocket engines.

Weber number is the ratio of the external flow's inertial forces to the droplet's surface tension forces, and is considered one of the most important determinants of how a droplet will breakup. The relationship between critical Weber number and the ratio of the flow's frequency to the droplet's natural frequency will be investigated for ratio values less than, equal to, and greater than one, which highlights the effect of a flow's frequency on the droplet breakup process. This project improved the meshing techniques of previous CFD models, validated certain numerical criteria, and developed a periodic velocity function for use in future models. This project began an investigation of two-dimensional droplet breakup and got initial results that compared well with the results of other computational studies. Future studies will expand upon these initial results and will consider the effect of the flow's phase on the droplet's breakup.

## 1 - Introduction & Background

Secondary droplet breakup plays a significant role in a number of different atomization and spray processes ranging from printing to fuel spraying in liquid-fueled engines. For example, secondary droplet breakup is considered an important component in combustion instability, which can lead to engine damage and failure, and reduced engine performance for a variety of liquid-fueled combustors such as rocket engines and jet engines. This example illustrates how studying secondary droplet breakup could potentially aid the development of important advances in engine technology, as well as advancements in other technical applications.

Secondary droplet breakup is the fragmentation and deformation of an initial droplet into smaller droplets or different shapes via some force. The breakup-inducing force can come from an external flow or a sound or pressure wave hitting the droplet. It is hypothesized that the breakup process will occur differently for external flows with different characteristics, such as steady versus time-varying flows. Both experimental and computational research projects have studied the breakup process for steady flows, and different breakup processes have been observed. Figure 1 illustrates how the droplet breakup process, or regime, changes as Weber number changes for steady flow [1].

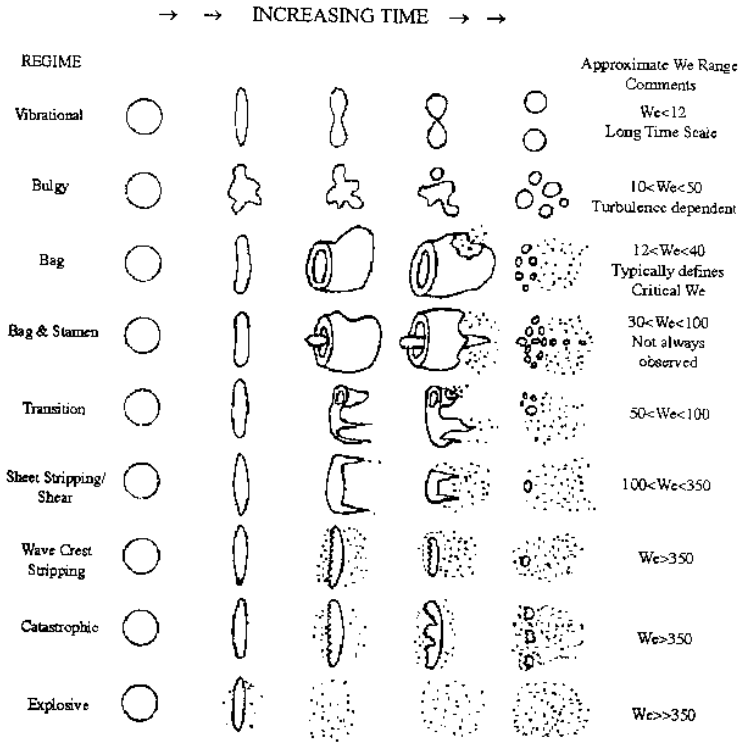


Figure 1. Secondary droplet breakup regimes for different approximate Weber number ranges [1].

This figure is a culmination of the breakup regimes reported by different research projects, and it is important to note that these projects have varying experimental apparatuses and initial droplet conditions. These experimental differences have led to varying reported critical Weber numbers, which is the combination of flow conditions at which the droplet begins the breakup process [1]. Weber number is defined by equation 1, and is the ratio of the external flow's inertial forces to the droplet's surface tension forces.

$$We = \frac{\rho d v^2}{\sigma} \qquad \text{Equation 1}$$

Where,

- $\rho$ = density of the flow fluid.
- $d$ = droplet diameter.
- $v$ = velocity of the flow fluid.
- $\sigma$ = droplet surface tension.

This dimensionless number is considered “the most important factor controlling the process of drop breakup…” [1]. As Weber number increases, the droplet becomes increasingly deformed by the flow’s inertial forces until the critical Weber number is achieved [1]. Figure 1 illustrates how complex this deformation process is, even for a steady flow. This research project adds another level of complexity by exploring the breakup process in flows that are time-varying. Time-varying flows are more representative of the flow conditions in certain atomization settings, such as within combustion chambers in engines, than steady flows are. The difference between these two flow situations will be explained in greater detail in the next section. Most of the research to date on secondary droplet breakup has been for steady flow situations due to the difficulties of experimentally modeling and analyzing the breakup process in periodic flows for a large range of flow conditions. This project aims to increase the knowledge and understanding of the field of secondary droplet breakup, specifically in periodic flow conditions that have not been studied before.

## 1.1 - Related Timescales of Steady and Periodic Flows

When considering secondary breakup, it is important to consider a couple different timescales associated with that process.

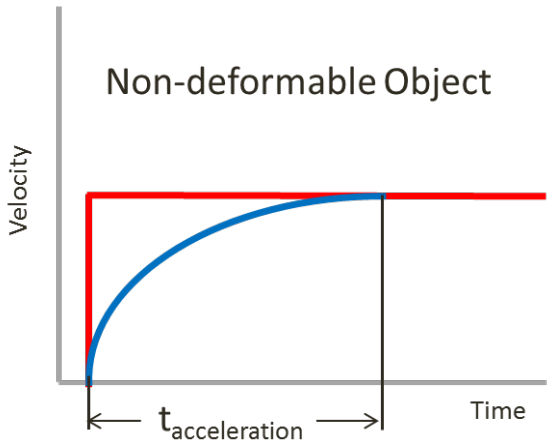


Figure 2. Response of a non-deformable object subjected to a steady flow.

Figure 2 illustrates a typical timescale related to an experiment where a non-deformable object is dropped into a steady flow. The red line is indicative of the velocity of the flow passing over the object and the blue line is the object's velocity history. At this point it is important to note what is meant by steady flow. The traditional definition of steady flow is that the properties of the flow, such as velocity, do not change with time. However, it is dangerous to use this term in reference to droplet breakup because nothing about the breakup process is actually steady. It is an inherently unsteady process. In the situation illustrated in Figure 2, the only thing that is steady is the velocity of the flow that the object is in. It is easy to see that the object does not act in a steady manner and accelerates to match the flow. *When the term "steady flow" is used in this report, it implies that flow over the droplet or object is unchanging with time, not that the response of the droplet is steady.* The important timescale in the situation of Figure 2 is $t_{acceleration}$, or the amount of time it takes for the object to accelerate from rest to the free-stream velocity. This timescale is quantified by equation 2 [1].

$$t_{acceleration} = \frac{4}{3}\frac{1}{C_d}\sqrt{\frac{\rho_d}{\rho_c}}t^* \qquad \text{Equation 2}$$

When the object is deformable a new timescale is introduced, which is $t_{breakup}$, or the amount of time it takes for the droplet to fragment, assuming it actually does breakup. Within $t_{breakup}$, there are a number of other important timescales that have been discussed in other research projects. These will be discussed more in section 1.2 "Steady Flow Studies". Figure 3 illustrates the typical response of a deformable object dropped into a steady flow.

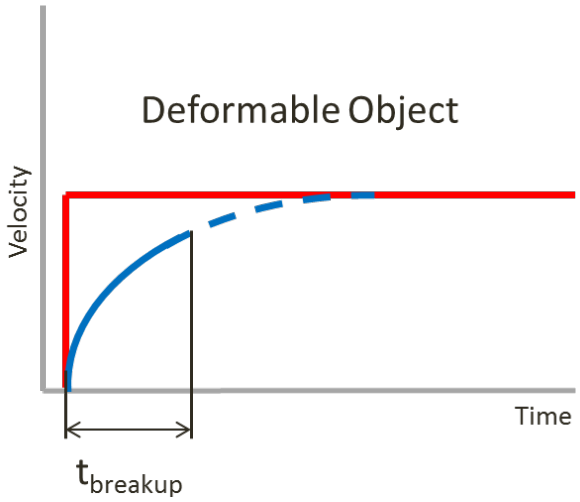


Figure 3. Response of a deformable object subjected to a steady flow.

Once the droplet or mass of fluid has accelerated to the flow's velocity, the relative velocity between the fluid and external flow is zero, obviously. At this point there is no inertial force applied on the fluid. It may seem that $t_{breakup}$ must always be shorter than $t_{acceleration}$ for the droplet to breakup, but it is possible for the droplet to breakup even after it has reached the free-stream velocity. The droplets in this situation have obtained enough energy from the flow that they will breakup even if it accelerates to match the external flow.

Periodic flows have additional timescales to consider. The frequency of the periodic flow dictates how quickly the flow changes from its minimum velocity to its peak velocity. A non-deformable object in a periodic flow with a low frequency will behave in a quasi-steady fashion. For example, if the flow takes several hours to reach its top velocity, the object will have no trouble matching the velocity of the flow. It will be able to accelerate and decelerate easily with the surrounding flow, and it is acceptable to treat the object as if it were in steady flow. A droplet in this scenario should breakup the same as it does in steady flows. However if the flow's frequency increases, at a certain frequency the object's velocity will not be able to match the changing velocity of the flow. At this point the relative velocity between the external flow and object increases, which increases the inertial force on the object. It is hypothesized that the

breakup process will vary depending on how high or low the flow frequency is. The distinction between a "high" and "low" flow frequency is explained subsequently.

The natural frequency of a droplet is the frequency at which the droplet will oscillate after it has been disturbed or set in motion, and is defined by equations 3 and 4 [2,3].

$$T_{NF} = 2\pi\sqrt{\frac{\rho_d d_d^3}{64\sigma}} \quad \text{Equation 3}$$

$$f_n = \frac{1}{T_{NF}} \quad \text{Equation 4}$$

Where,

- $\rho_d$ is the density of the droplet
- $d_d$ is the droplet's diameter.

It is hypothesized that the difference between high and low flow frequencies is determined by the droplet's natural frequency and whether the flow's frequency is higher or lower than it. This relationship between the droplet's natural frequency, the flow's frequency, and critical Weber Number is one of the primary focuses of this project, and future related projects. *Secondary Droplet Breakup in Periodic Aerodynamic Flows* presents the following hypotheses about this relationship, which this current project will test [1]:

- When the flow's frequency is small compared to the droplet natural frequency, the droplet will respond as though exposed to a steady flow.
- When the flow's frequency is much larger than the droplet natural frequency, it is predicted that the droplet will respond primarily to an appropriate average velocity.
- When the flow oscillation frequency closely matches the droplet natural frequency, there will be a complex droplet response.

Future projects will also study how the flow's phase affects the breakup process. It is hypothesized that the phase of low frequency flows will have a larger impact on the breakup process than high frequency flows will. For flows that take longer to change from the minimum velocity to peak velocity, it will be important whether the droplet is subjected to the minimum or peak velocity first. This is because the breakup process might complete itself before the flow changes velocity. The process might also depend on whether the flow velocity is increasing or decreasing once the droplet is subjected to the flow. As mentioned above, there is very little data or analysis available on breakup in these kinds of flows.

## 1.2 - Steady Flow Studies

A large amount of literature is available on secondary droplet breakup in steady flows from both experimental and computational research projects. The experimental apparatuses used in these experiments are typically drop towers or shock tubes, and the computational studies tend to focus on the atomization of several droplets. Many of these studies use experimental data to model the droplet breakup processes, which provides little help for comparison with the results from this project. It is important to note that this section on Steady Flow Studies is an incomplete overview of the available research on secondary droplet breakup in steady flow.

Dr. G. Faeth [Union College '58, 4] from the University of Michigan has a number of articles that discuss the secondary droplet breakup processes, and summarizes the work of other researchers. Faeth describes that the effect of viscosity on the breakup process is negligible for Ohnesorge Numbers $< 0.1$, at which point Weber Number dictates the breakup process [1]. In these flow conditions, the droplet oscillates with an amplitude that is weakly dampened by its viscosity [5]. For higher Oh, both critical Weber Number and the transitions between different breakup regimes occur at higher values than for low Ohnesorge Number values [1]. What happens is that the increased droplet viscosity increases the damping effect of the droplet's

oscillations, and thus impedes the breakup process. When the Ohnesorge Number gets high enough, the oscillations are eliminated completely. Consequently, this viscosity effect dampens the formation of bag and bag and stamen breakup regimes, which leaves only shear breakup as the remaining regime [5]. As mentioned earlier, this oscillating nature of the droplet may play a significant role in the droplet breakup process in periodic flow, so it is important to understand this relationship before exploring even more complex scenarios.

Faeth explains that the "effect of wide variations of surface tension and liquid to gas ratio on secondary droplet breakup properties must be known in order to address practical applications." Up to this point in time, experiments have been limited to liquid to gas ratios greater than 500 and Reynolds Number greater than 50 [5]. "…the objective of computations of drop deformation (is) to consider the response of drops to…the small liquid to gas density ratio, large Ohnesorge Numbers and smaller Reynolds Number conditions that are difficult to address by experiments but are more representative of conditions in sprays at the pressure typical of practical power and propulsion systems [5]." The Ohnesorge Number is the ratio of droplet's viscosity force to surface tension force and is defined by equation 5 [1].

$$Oh = \frac{\mu}{\sqrt{\rho_d * d_d * \sigma}} \qquad \text{Equation 5}$$

Where,

- $\mu$ is the viscosity of the droplet fluid.

It is obvious that additional information is necessary to understand droplet breakup processes even in steady flows. The capabilities of computers and supercomputers today allow for computational studies of situations that are impossible or very difficult to model with experiments, which is one of the underlying intentions of this project.

Faeth discusses the results of a computational analysis of droplet deformation that studied the effects of We, Oh, Re, liquid to gas density ratio, and liquid to gas viscosity ratio on the deformation process. This study first conducted different basic simulations and compared them to experimental results. These simulations included comparing the wake characteristics behind a non-deformable sphere to Re, comparing the $C_D$ over the sphere to the flow's Re, and the maximum droplet deformation as a function of Weber Number between 2 and 13. The computational results of these cases agreed with experimental results, and were "well within computational accuracy and experimental uncertainties [5]." A similar verification case is tested in this study to make sure that Star-CCM+ can be used correctly to model even simple cases, and is explained later in section 4 - Marble in Steady Flow. The significance of this is that modern CFD software can be used to accurately model these types of drop breakup processes. As long as the computational models in this project are setup correctly, it is reasonable to assume that they will provide useful information that can be used to increase knowledge in this field.

Schmehl, Maier, and Wittig (2000) produced a CFD analysis of fuel atomization, secondary droplet breakup, and spray dispersion, specifically for the fuel and air mixture process in a combustor. This CFD model used a coupled flow model and a Lagrangian droplet tracking method to model the individual droplets, which are different than in the models for this project. Although this article does not focus specifically on secondary droplet breakup, it provides interesting information on the different shapes and sizes the droplet experiences, and how quickly these changes occur for different breakup regimes. This project compared experimental data of the atomization and breakup processes to computer simulation results [6].

Similar to what is reported by Bruno [1], they report that the first phase of bag and bag and stamen deformation is the droplet flattens out and its diameter increases. Schmehl, et al. provides a correlation for the maximum diameter value, as described by Equation 6.

$$D_{max} = D_0(1 + 0.19 * \sqrt{We}) \quad \text{Equation 6}$$

Where,

- $D_0$ is the droplets initial diameter.

In the second phase of bag and bag and stamen breakup regimes, the balloon shaped portion of fluid expands to between six and seven times the droplet's original diameter. In the shear breakup process, the droplet size is reduced to a maximum stable diameter, which results in a constant drag coefficient. The article provides a correlation to approximate the drag coefficient on the droplet for Weber numbers below the critical Weber number [6]:

$$C_D = 0.28 + \frac{21}{Re} + \frac{6}{\sqrt{Re}} + We\left(0.2319 - 0.1579 * \log(Re) + 0.0471 * log^2(Re) - 0.0042 * log^3(Re)\right)$$

Equation 7

This article failed to mention which breakup regimes this correlation applies for. However, the drag forces experienced by the droplet is of utmost importance to this project, so it is important to understand as much as possible about what forces it may experience.

Both Dr. Bruno from Union College and Schmehl, et al. each discuss the significance of specific timescales in the breakup process. This was briefly mentioned before, but will be discussed more in-depth now. Table 1 contains a couple examples of reported breakup timescales with descriptions [1].

Table 1. Breakup times presented in different literature.

| Name | Symbol | Description |
|---|---|---|
| Drop Deformation Time | $t_{def}$ | Time required to flatten the droplet to some diameter |
| Initial Breakup Time | $t_i$ | Time when first fragments separate from initial drop |
| Primary Breakup Time | $t_p$ | Time at which initial droplet no longer coherently exists |
| Final Breakup Time | $t_b$ | Time at which there is no more breakup of initial droplet or daughter fragments |

Bruno notes that for some regimes, $t_p$ and $t_b$ may be the exact same length of time. The different breakup time values are normalized by equation 8.

$$t^* = \frac{d_0}{U_0}\sqrt{\frac{\rho_d}{\rho_c}} \qquad \text{Equation 8}$$

This timescale is the time it takes for the droplet to be flattened into a disk, which is defined by the same relationship for all breakup regimes [6]. Bruno explains that because $t^*$ has an influence in boundary layer growth, instability growth, and "the initial stages of drop deformation and flattening," it is expected that $t^*$ is "an important scaling parameter over a very wide range of Weber Number and breakup regimes [1]." This parameter is an important indicator of how long it takes for the droplet to reach breakup, and thus how long it takes for the simulations to run. Due to time constraints with this project, it is important to minimize the amount of time each simulation takes to complete. Thus, t* is kept as small as possible within these simulations. This is explained more in section 1.5 – Dimensionless Numbers.

There are a number of different empirical correlations for the breakup times in Table 1 for different droplet and flow conditions. For a summary of these correlations with explanations, see section 2.5 in *Secondary Droplet Breakup in Periodic Aerodynamic Flows*.

## 1.3 - Periodic Flow Studies

There is minimal research available on droplet breakup in periodic flows, and the most relevant research is the work of Bruno in *Secondary Droplet Breakup in Periodic Aerodynamic Flow*. The hypotheses of droplet breakup in periodic flows stated in section 1.1 - Periodic Flow and Related Timescales are from Bruno. This project is an extension of his work and will investigate these hypotheses further. Bruno was unable to produce certain periodic flow conditions experimentally, but with CFD it is possible to model these complex flow conditions, as long as they are modeled correctly. This project develops certain tools and methodologies for

producing models that are numerically correct and capable of accurately modeling periodic flow conditions. With the help of future students, this project will hopefully shed light on an important fluid mechanics topic that has little research available to date.

## 1.4 - Previous Work

This research project is a continuation of Krystle Gallo's senior project from the academic year of 2011-2012 [3]. This current research project referenced the same simulation models that Gallo used in her project. The general shapes of bag and shear breakups in Gallo's models matched those described in *Secondary Droplet Breakup in Periodic Aerodynamic Flows* very well (see Figure 1). There is a concern with the diffusion of the droplet's liquid into the surrounding flow. However, this can be altered by changing a sharpening factor in the Volume of Fluid multiphase model and changing the underlying mesh, which will be discussed in future sections. Before she graduated, Gallo began to model some periodic flows and got initial results that were similar to what has been hypothesized, as stated in section 1.1 Related Timescales of Steady and Periodic Flows [7]. However, these results are limited in their accuracy and were more of a proof of concept that Star-CCM+ can be used to model this phenomenon. Some of these results are illustrated in Figures 7 and 8.

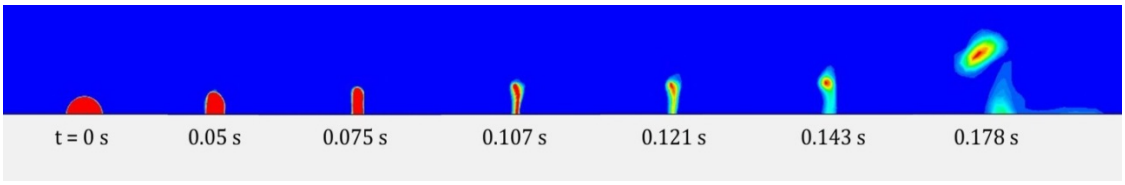


Figure 4. Steady Flow Case with We=12 and Bag Breakup

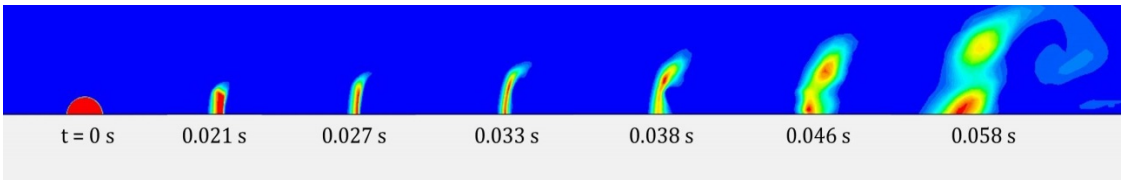


Figure 5. Steady Flow Case with We=100 and Shear Breakup

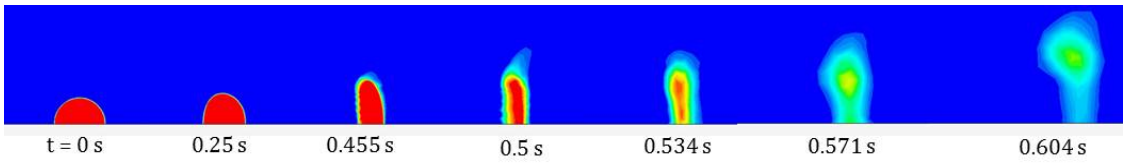


Figure 6. Periodic Flow Case with We=12 and ω=2.23534.

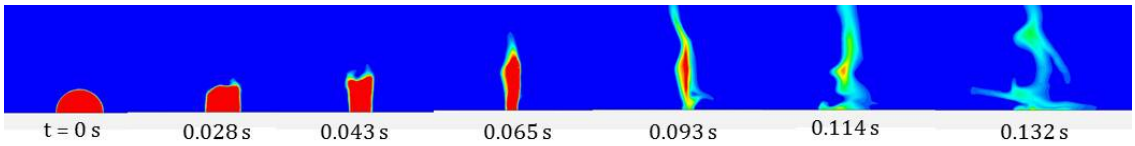


Figure 7. Periodic Flow Case with We=12 and ω=24.3534

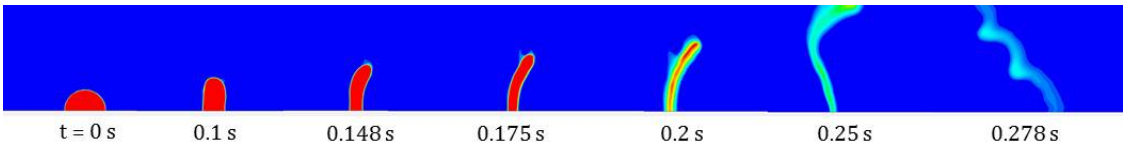


Figure 8. Periodic Flow Case with We=12 and ω=243.534

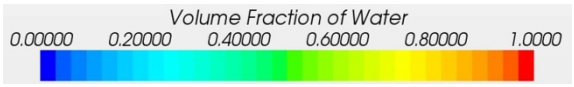


Figure 9. Volume Fraction of Water Scale for All Steady Simulations

The periodic simulations with a flow frequency less than the drop's natural frequency were similar to the results for a steady flow at the same We, which was expected. For example, it is easy to see that the deformation process in Figure 6 is similar to the bag breakup in Figure 4. The results of simulations with a frequency close to the drop's natural frequency were somewhat complex, but had characteristics similar to those of a shear breakup. The edges of the droplet bent in the downstream direction, similar to shear breakup, and then bent the other direction when the flow changed directions. The results of tests for a frequency greater than the drop's natural frequency were very complex, as shown in the right most images of Figure 8. Gallo's simulations raise a question about the nature of the periodic function that she used for the flow velocity in these models. Her function oscillated from a positive velocity and to a negative velocity of the same magnitude. The other way the velocity function could operate is to oscillate between a higher positive velocity and a lower positive velocity. In situations such as a combustion

chamber, the sound waves will pass through the droplet and continue in the same direction. It will not pass through the droplet, change direction, pass through it again, and continue to change back and forth. A periodic velocity function was produced in this project that more accurately represents a pressure wave passing through the droplet, which is explained in more detail in section 2.5 - Periodic Velocity Function.

## 1.5 - Dimensionless Numbers

As with any fluid dynamics situation, there are a number of dimensionless numbers that are important to secondary droplet breakup. Although this study does not consider an exhaustive list of dimensionless numbers for this situation, it does take into account the following in Table 2. This table includes a couple other parameters that are important to this experiment, but are not dimensionless [1, 8].

Table 2. Important dimensionless numbers and parameters for Secondary Droplet Breakup.

| **Dimensionless Number** | **Definition** |
|---|---|
| We, Weber Number | $\frac{\rho_c * d_d * (U_c - U_d)^2}{\sigma}$ |
| Re, Reynolds Number | $\frac{\rho_c * d_d * U_c}{\mu_c}$ |
| Oh, Ohnesorge Number | $\frac{\mu_d}{\sqrt{\rho_d * d_d * \sigma}}$ |
| t* | $\frac{d_d}{U_2}\sqrt{\frac{\rho_d}{\rho_c}}$ |
| $T_{NF}$, Droplet's Period of Natural Frequency | $2\pi\sqrt{\frac{\rho_d * {d_d}^3}{64 * \sigma}}$ |
| C, Courant Number | $T_{step} * \frac{U_c}{dx}$ |

An important capability to have with these experiments is to change only Weber number while keeping the other dimensionless numbers and important parameters the same. This allows the

results of different simulations to be compared due to the similar fluid situations in which they take place. This can be difficult considering these numbers contain variables that overlap with each other. Due to the following relationship, it is impossible to change Weber number without keeping both t* and $T_{NF}$ the same.

$$\frac{t^*}{T_{NF}} \propto \frac{1}{We^{0.5}} \qquad \text{Equation 9}$$

Because t* plays an important role in how long it takes a droplet to breakup, and how long it takes for simulations to complete, $T_{NF}$ is allowed to float while keeping t* constant. The methodology used to change Weber number while keeping the other parameters the same consists of two steps:

1. Change surface tension, $\sigma$, to change Weber number.
2. Change the droplet's dynamic viscosity, $\mu_d$, to change Ohnesorge Number back to its initial value.

$T_{NF}$ is affected by the droplet's surface tension, so it will change as Weber number changes. These experiments will be replicated with the same dimensionless number values and with t* allowed to float while $T_{NF}$ is held constant, to see which parameter has a larger impact on the breakup process.

As mentioned in 1.2 – Steady Flow Studies, Faeth presents important information on Ohnesorge Number and the effects of the droplet's viscosity for Ohnesorge Number values greater than 0.1.

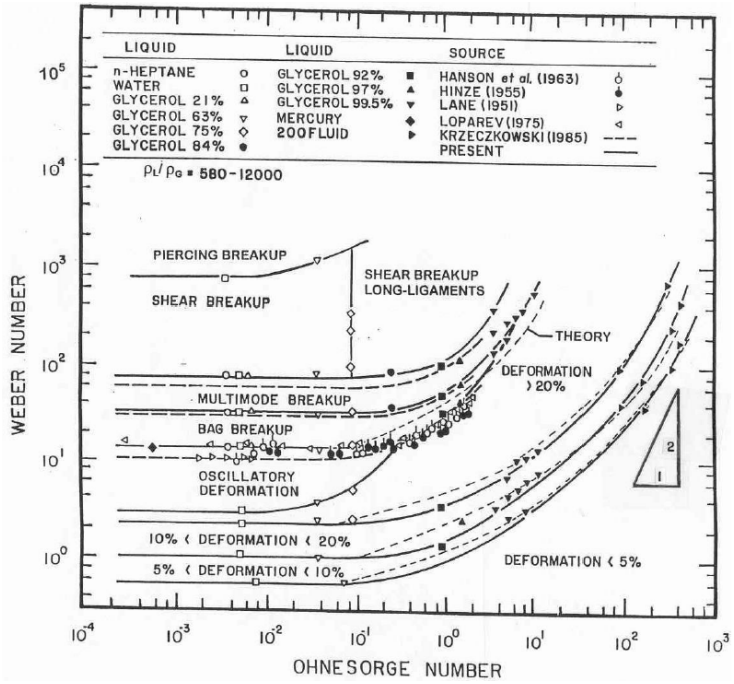


Figure 10. Relationship between Oh and We for different breakup regimes [5].

Figure 10 illustrates that critical Weber number is unaffected for Ohnesorge Numbers less than 0.1, whereas it increases for values above 0.1 due to the dampening effect of the increased droplet viscosity. Because of this relationship, the Ohnesorge Number is held below 0.1 for all simulations.

## 2 - Star-CCM+ Model

The computational fluid dynamic software used in this project is Star-CCM+ Version 7.04.006, which is from the company CD-adapco. To save computer memory, our model utilized a two-dimensional, axisymmetric model for both the droplet and the solid sphere for the marble test case, which is explained in section 4.1 - Marble in Steady Flow. It was assumed that due to the symmetry of the droplets and sphere, only half of the object could be modeled and the CFD program would still produce useful results. Because the mesh was converted to a two-dimensional model, these models simulate only half of a cross-section of the droplets and sphere. These methods reduce the amount of computer memory used, which also reduces the amount of

time it takes for the simulations to run. It is important to note that this assumption eliminates important physics, but the computational and time limitations of this project do not allow for a full model of the breakup process. This project is a step towards completely modeling droplet breakup with CFD, and it is essential to acknowledge the limitations of the models used. The limitations due to the axisymmetric assumption are similar to those discussed in 4.1 - Marble in Steady Flow for the solid sphere. The process used to discretize the solution domain geometry, and the physical models used to model the droplet are explained subsequently. These simulations were setup to record an image of the droplet after each time step. Movie Maker from Microsoft was used to compile these images and produce a video of the droplet deformation, which were very useful for visualizing the breakup process.

## 2.1 - Meshing

One of the most important aspects of these simulations is meshing the geometry, or solution domain, that contains the sphere or droplet. The cells in a mesh are what the software program uses to calculate the flow properties in a certain area of the geometry. It is important to note that the program treats everything within one mesh cell as uniform in terms of the flow calculations, which illustrates the importance of a refined mesh. Creating a proper mesh in a simulation can take a long time to setup, and for the program to actually create. One of the most time-intensive aspects of meshing is assessing the tradeoff between accuracy, numerical stability, and computational cost [8]. The more dense the entire geometry is, the more accurate the solution is because the smaller cells will be able to model details of the flow that coarse meshes would miss. However, denser meshes require more computer memory, which results in longer simulation times and the necessity for powerful computers [8]. One method to handle this issue is to differentiate the mesh density in different portions of the geometry to improve the quality of the results in the areas of interest, and reduce the mesh density in the areas where minimal

activity is occurring. Finding out which areas are of most interest requires running a number of simulations and then studying the results to determine where the most activity occurs.

Numerical stability depends in part on how distorted the individual mesh cells are. The program can model flow between different cells with less error if the cell shapes are closer to general geometric shapes, such as squares or triangles. For complex geometries, it is difficult to model the entire geometry in terms of general shapes, so errors can occur between the interfaces of complex mesh cells. Increasing the mesh density helps reduce the effects of these errors, but requires more computational memory, as mentioned before [8]. This process requires several iterations of different simulations with different mesh densities and orientations before deciding on an acceptable mesh.

Before meshing can begin, the solution domain geometry must be imported into the program. The initial geometry was an eighth section of a tube, as shown in Figure 11.

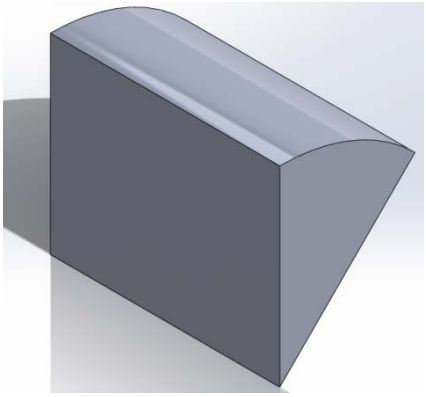

Figure 11. Initial model geometry.

The first step of meshing is selecting the meshing models provided by Star-CCM+, and choosing the reference values for each model. The meshing models chosen for these models include surface remesher, polyhedral mesher, and prism layer mesher. The base size, which is the reference length value for both surface and volumetric mesh cells, was set at either 0.001 m or 0.005 m. The relative minimum surface size was set to 100% of the base size, the relative target

size for the largest cells was 500% of the base size, and the prism layer thickness was set at 100% of the base size [3]. To create a denser mesh around the droplet or sphere, or in the areas where most of the important activity occurs, a volume shape was created that encompassed those areas. This shape was made in the tools section of Star-CCM+. The dimensions of these volume shapes are yet to be determined for periodic flow models because the high interest areas of droplet deformation in these flows are still unknown. However, Gallo's results in Figure 4 and Figure 5 provide information on the areas that the droplets deform to in steady flows.

The next step in the process is surface meshing the geometry, which breaks the surface of the whole geometry into small geometric pieces. Even though this model uses a two-dimensional strategy to simulate the droplet, Star-CCM+ requires a three-dimensional volumetric mesh before converting to two-dimensional, so extra time was taken to produce a volumetric mesh. This mesh breaks up the entire volume of the geometry into smaller shapes, and takes much longer than the surface meshing to complete. It uses all of the same base and reference values that the surface mesh used. Once the volumetric mesh was finished, it was converted to a two-dimension mesh. An example of a two-dimensional mesh used in these simulations is shown below.

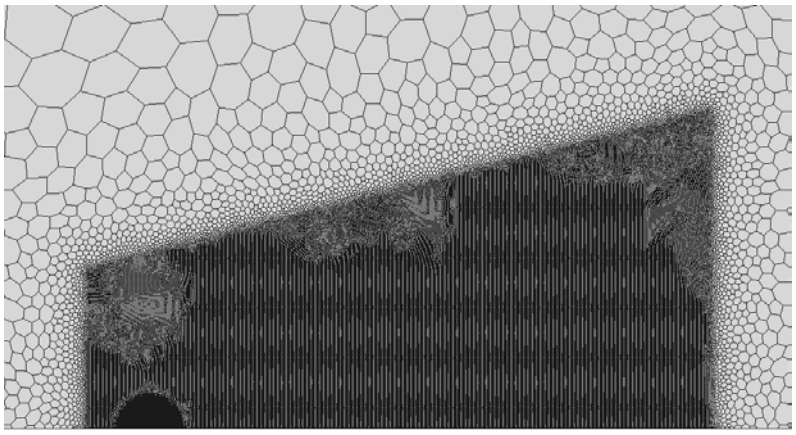

Figure 12. Example of a two-dimensional mesh.

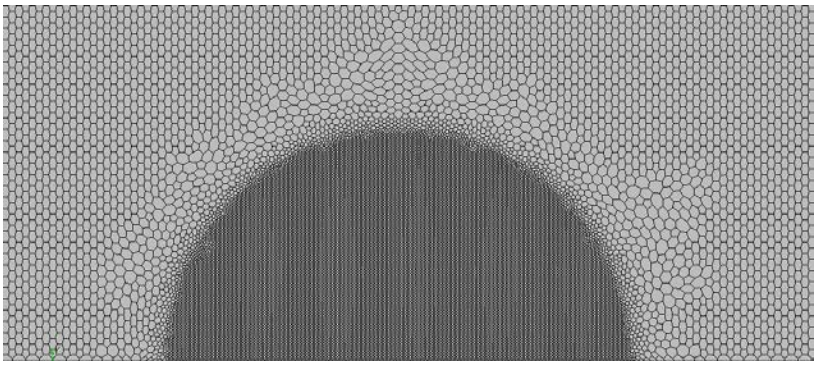

Figure 13. Close-up view of two-dimensional mesh around the initial droplet location [3].

The different settings and sizes used for each mesh are tabulated below. These mesh types correspond to those visualized in Table 3. The Hemisphere and Extended/Frustum columns provide the relative size of the cells within the hemisphere shaped mesh areas and those extending behind the hemisphere, as a percentage of the base size.

Table 3. Mesh settings for different mesh types.

| **Mesh Type** | **Base Size (m)** | **Hemisphere (% of base size)** | **Extended/Frustum (% of base size)** |
|---|---|---|---|
| A | 0.005 | N/A | 2.5 |
| B | 0.005 | 2.5 | 10 |
| C | 0.005 | 2.5 | 10 |
| D | 0.005 | 2.5 | 7.5 |
| E | 0.005 | N/A | 15, 25, 40 |
| F | 0.001 | 20 | N/A |

## 2.2 - Physical Models

As mentioned earlier, the initial geometry incorporates an axisymmetric model of the droplet, so the axisymmetric physics model was chosen with the x-axis as the axis of symmetry. Gallo notes that “with a non-spherical initial droplet, this (physics model) would not be applicable” and that “any non-axisymmetric effects are lost from the simulation [3].” Because the droplet breakup process is inherently unsteady, the implicit unsteady model was selected [3].

There are two methods used to solve the Navier-Stokes equations: coupled and segregated. This model utilizes the segregated method, which solves the momentum and continuity equations separately, as opposed to the coupled method, which solves these at the same time [9]. The segregated solver is good for incompressible flows, which this project assumes, and uses less computer memory than the coupled method [10]. This physics engine requires a corresponding heat transfer model, which is the segregated fluid isothermal model. The use of the segregated model allows for the use of the volume of fluid to model the multiphase flow, which is explained in more detail later in this section. Gallo reports that the Reynolds Number "for the various flow velocities (in these simulations) was calculated to range from 6330 to 53800, allowing the laminar physical model to be chosen." Turbulent flow over a sphere begins around a Reynolds Number value of 200000 [11]. Gravity was ignored in these simulations to eliminate forces not caused by the external flow. Gallo notes that "surface tension, which is a very important aspect of droplet-air interaction, was modeled through a Multiphase Interaction Model, with air as the primary fluid and water as the secondary fluid." Gallo produced the initial multiphase situation by creating two Eulerian phases under the Eulerian multiphase tab. The first phase was water modeled with constant density, and the second was the air, which was modeled as an ideal gas. To define the initial shape and location of the droplet, a field function was created [3]:

($$Centroid[1]<=(sqrt(0.0001-pow(($$Centroid[0]-0.5),2))))&&($$Position[1]>0)?1:0

Equation 10

Gallo explains, "the code reads: if the y value of the geometry is less than or equal to $\sqrt{0.0001-(x-0.5)^2}$ and the position is above the x-axis, then the value is 1 (water), else the value is zero (air)" [3].

## 2.3 – Volume of Fluid (VOF)

When dealing with multiphase flows, it is very important to model the interface between the different fluids as accurately as possible to correctly apply boundary conditions between the fluids. There are a couple of different methods for modeling this interphase such as Lagrangian dispersed phase, algebraic slip, Eulerian, Eulerian granular, and volume of fluid (VOF) [12]. These different methods have specific advantages and disadvantages, and some models are better for different tasks than for others. The method used in this project is VOF, which is a "front-capturing" method and is described as a good model for situations where each phase makes up a large structure and there is minimal contact area between the phases [13, 3]. For example, VOF would not be well suited for a situation where there are many droplets in a flow [3]. This model works by defining a marker function that is a value of one for any mesh cell that contains only a specific fluid, and a value of zero for any point that does not contain any amount of that fluid.

$$H(x) = \begin{cases} 1, if\ x\ is\ in\ fluid \\ 0, if\ x\ is\ not\ in\ fluid \end{cases} \qquad \text{Equation 11 [12]}$$

The marker function can be based off the difference in a fluid property such as density or viscosity between the two fluids [13]. Whereas "front-tracking" models utilize marker particles, which are points that move with the fluid velocity at its particular location, VOF requires only one value per cell. This saves the computer from storing the location of multiple points and calculating where they move to next. Any cell with a value between zero and one indicates a cell that contains a surface. The method used to define the surface between the fluids varies for different forms of VOF models, but the more-accurate methods "reconstruct" the surface in each cell based off the value of the marker function, H [13]. The piecewise linear interface calculation (PLIC) method is a higher order method that creates a line segment in the cell that is perpendicular to the gradient of H in that cell (the direction of the quickest changes in H). The ends of these line segments do not necessarily match up with the segments in adjacent cells, but

they are close to matching. The program then reconstructs this interface line and makes the lines in adjacent cells connect. With this estimated interface, the program sets boundary conditions for the fluids and assesses how they change next [14].

The color function, C, is the average value of H in each mesh cell and is used to define a color value or shade for that particular cell:

$$C_{i,j} = \frac{1}{\Delta x \Delta y} \int_V H(x,y)\, dx\, dy \qquad \text{Equation 12 [13]}$$

Cell-averaged marker functions tend to have an issue when they move from one cell to the next in that they experience numerical diffusion, which results from the program rounding flow calculations. This diffusion process results in several mesh cells partially filling up with both fluids and smudging the surface between the two fluids. One way to handle this is to increase the Volume of Fluid Sharpening Factor, which makes the interface between the two fluids more defined. Increased interface sharpening is recommended in surface-tension dominated flows, however additional sharpening of the interface can lead to "non-physical alignment of the free surface with the grid lines" [10]. A simulation was run to test the effect of large sharpening factors. The results illustrated the danger of using factors that are too large, and are explained in more detail in section 5.4 – Simulations of Drops in Periodic Flow.

## 2.4 - IBM Intelligent Cluster

Union College now has an IBM Intelligent Cluster, which is available for research projects such as this one. This system will be utilized more in future projects for things such as meshing and running actual simulations. Gallo tested the benefits of using this system by timing how long it took the same simulation to run on a regular lab computer in Union's Mechanical Department versus on the Intelligent Cluster. She found that the simulation took 7 hours and 42 minutes to run on the department computer, and only 55 minutes on a small portion of the

cluster's full computing power. With this computing power available, recording data from simulations of periodic flow should progress quickly in future projects. Certain problems presented themselves during this project that limited the amount that the IBM Intelligent Cluster was used.

## 2.5 - Numerical Criteria Testing and Validation

Due to the nature of CFD software, certain numerical criteria must be satisfied in order to produce accurate solutions. Two criteria that are particularly important to these time-varying flow simulations are Courant number and the Nyquist sampling theorem. These types of simulations include changes in flow across space and time, which Courant number and the Nyquist sampling theorem consider, respectively. Ms. Gallo's simulations of steady flow droplet breakup did not take into account these criteria, whereas this project does. Validating the work prior to this project is one of the primary objectives of this research project.

One of the most important numerical conditions to satisfy with any CFD simulation is Courant number, which takes into account the time step used in the flow calculations, the flow's velocity, and the size of the mesh used to discretize the solution domain.

$$C = \frac{U_c \cdot T_{step}}{dx} \qquad \text{Equation 13 [8]}$$

Rearranging Equation 13 for $T_{step}$ states that the time step should equal the time it takes for the flow to cross one mesh cell, times a constant, C. [8]. This constant is the Courant number, and is allowed to vary from above zero to five for the implicit scheme used in these simulations [8]. Due to variations in the mesh cells throughout the solution domain, dx is defined as the smallest length found in all of the mesh cells that is in the direction of the flow. In the interest of minimizing the length of time of each simulation, $T_{step}$ is kept as large as possible to decrease how long it takes the solution to reach breakup. This requires a smaller free-stream velocity for a

given mesh, or dx. For a time step of approximately 4E-4 seconds, a dx of 5.90E-5 meters, and a velocity of 1m/s, the Courant number is approximately three, which is within the requirements of the implicit scheme.

The Nyquist sampling theorem states that to accurately sample a function, the sample rate must be at least twice as often as the function's maximum frequency [8]. This has implications for the periodic velocity function in this simulation. If the velocity function's frequency increases, the time step needs to decrease in order to capture the quicker velocity changes. The time step, which is synonymous to the sampling rate in these simulations, should be at least ten times smaller than the velocity function's frequency. Because there are two different criteria that can determine the time step used in these models, the smaller of the two will be used to satisfy both criteria.

## 2.6 - Periodic Velocity Function

Validation tests were conducted to ensure that the periodic velocity function performs as intended. The periodic velocity function is defined at the domain's inlet and not throughout the entire domain, which can lead to issues such as varying velocities values from one area to another in the domain. If the velocity's frequency is high enough, the velocity may change before the flow is able to move through the entire domain. Due to the incompressible physics condition, the velocity should not change across the domain, but tests were run to make sure the flow velocity within the solution domain does in fact change all together.

The solution domain for these tests was made to the same size and dimensions as the simulations with the droplet, but the droplet was not put into the domain. In order to save time and computational memory, the mesh in this version was less refined than the one in the droplet simulations. A monitor of the inlet's velocity and a corresponding plot were used to verify that

the velocity function reached the prescribed maximum and minimum values and fluctuated as it was supposed to, as shown in Figure 14.

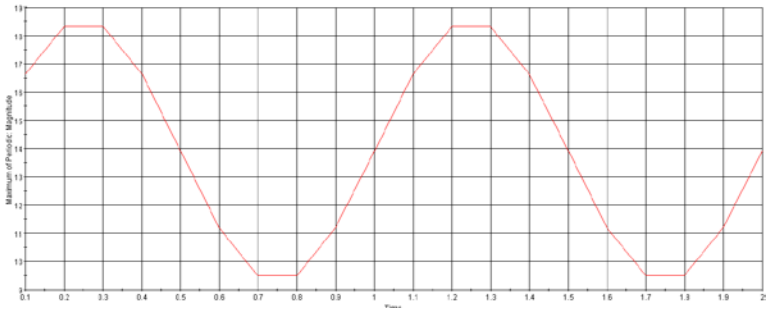

Figure 14. Periodic velocity at solution domain's inlet.

A scalar scene was used to visualize the velocity throughout the domain. Pictures of the velocity were documented after each time step and these were checked visually for any inconsistencies in the velocity throughout the entire domain.

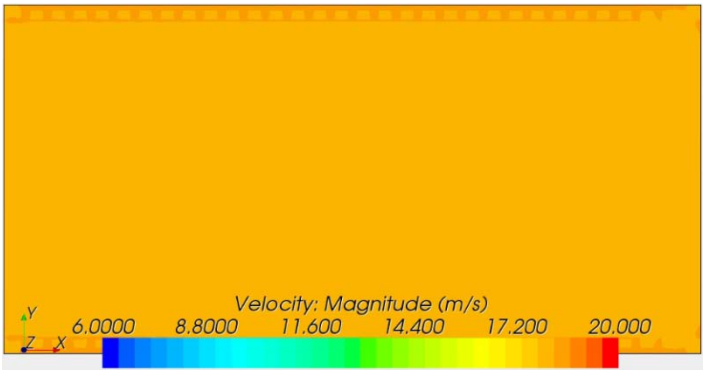


Figure 15. Example of color diffusion at the top of the solution domain.

Figure 15 illustrates one image from this test. At very high frequencies ( 1000 hz), there are a few areas along the top of the solution domain that have different velocities than the rest of the domain, however these are not too much of a concern. These areas differ by only one color value from the rest of the field, which implies that the velocity may be between the two different color values at those locations. It is important to note that measuring the velocity with a color scale is imprecise. If there was a range of several different colors across the solution domain, there would be some concern because this would imply that there are in fact inconsistencies in the velocity, which is undesirable for these tests. No evidence of such a problem was found.

## 3 - Objectives

The objective of this overall project, including the work of Krystle Gallo and future students, is to determine the effects of periodic flows on droplet breakup. Gallo states that, "the scope of (this) project was to increase the fundamental knowledge about droplet breakup in an area that has not been heavily researched to date. With current computational power, it is now possible to represent complicated fluid dynamics situations on a computer for which experiments are not possible [3]." Through the use of Star-CCM+ on Union College's IBM Intelligent Cluster and Mechanical Engineering Department computers, these complex situations will be computationally modeled and analyzed.

Although this project was unable to simulate any droplet breakup in periodic flow conditions, different methodologies and components necessary for producing accurate simulations were developed. These developments include improved meshing techniques over those used in previous CFD models, validation of certain numerical criteria, and the development of a periodic function that works as desired for these tests. A few other objectives that future projects will complete, or consider, are the following. Some of these objectives were suggested in either *Secondary Droplet Breakup in Periodic Aerodynamic Flows using Computational Fluid Dynamics* [3] or *Secondary Droplet Breakup in Periodic Aerodynamic Flows* [1].

- Determining transitional Weber numbers between the different regimes for this CFD simulation [3].
- Analyze the sufficient time of action needed by the applied load to complete breakup and the effect on critical Weber Number due to loads with durations shorter than breakup time [1].
- Analyze the effect of loading rate on critical Weber Number and other aspects of droplet breakup [1].

The results from this project provide a pathway for future research projects that will provide new knowledge and understanding into the field of secondary droplet breakup.

## 4 - Marble Test Cases

A simple flow situation was modeled to make sure that we could correctly use Star-CCM+ to accurately model even basic fluid situations. The scenario tested was similar to the work Gallo produced, except that the object in steady flow was a solid sphere instead of a droplet. It is important to note that when this sphere is projected to a two-dimensional surface, it replicates a cylinder in cross flow. The process for setting up this simulation was similar to that of the droplet simulations except that a turbulent model was used instead of a laminar model, the steady model was used instead of the unsteady one, and there was no need for a multiphase model such as VOF. The turbulent physics model was used to model the flow on the downstream side of the sphere profile, which is inherently turbulent. The $C_D$ versus Reynolds Number relationship for a sphere profile in cross-flow is well known, and this experiment hoped to match this $C_D$ versus Reynolds Number data.

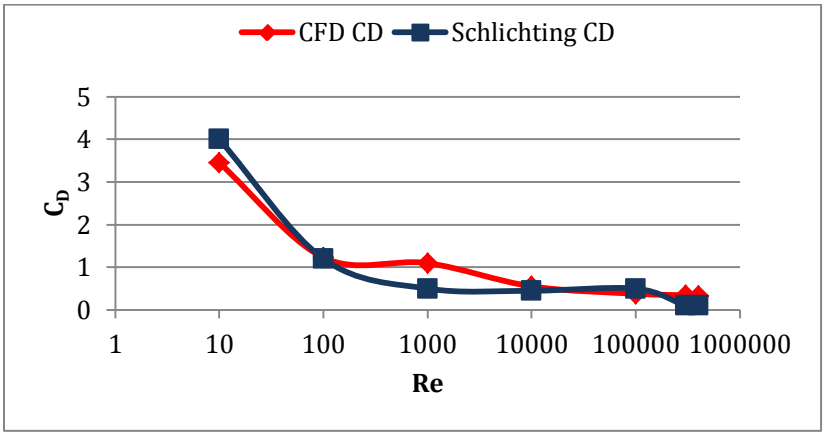


Figure 16. Computational drag coefficients versus experimental drag coefficients.

Figure 16 compares the data from the CFD simulation with certain points of the Schlichting $C_D$ versus Reynolds Number data, which is widely accepted as accurate and correct for cross-flow

over a sphere [11]. It is important to note some of the differences between the two data sets. At a low Reynolds Number value, the flow over the sphere profile is laminar. Because the CFD model used a turbulent model, this simulation most likely produced a lower $C_D$ value at the low Reynolds Number value. In real life around a Reynolds Number of 1000, there are vortices alternatingly shedding off both sides of the sphere, which is an unsteady process. However, since only half the sphere was modeled and the steady model was used, these results were completely eliminated. This simulation forced a steady solution, which is unrealistic. Around a Reynolds Number of 200000, the flow begins to transition to turbulent, at which point the boundary layer separates later from the sphere and the drag coefficient drops off suddenly. The CFD model was unable to account for the delayed boundary layer separation, so the program did not calculate any drop off in $C_D$. Overall, the results from this test agreed well with the accepted data and any areas of difference were easily explained. There was very good agreement for Reynolds Number values of 100 and between 10000 and 100000. These results imply that we can use Star-CCM+ correctly to model fluid situations that are similar to that of this project.

## 5 - Results Catalogue

Although this project did not complete its desired goal of modeling secondary droplet breakup in time-varying flows, it did produce several different simulations during the process of numerically validating the base CFD model. The results of these tests may not be correct, but they illustrate what has been tested and why it did not work. This catalogue presents the different test cases that were run, and any useful information about the simulation results and where the Star-CCM+ file can be located. In order to save space in the file's name, only the dimensionless numbers and parameters in Table 5 will be reported for each model. With the provided excel sheet [15], it is easy to plug in the property values from each simulation and find other useful information about that test case.

## 5.1 - File Labeling

The label of each simulation file is intended to provide enough information about the test case that nearly every important characteristic can be determined by the information in the file name. Certain dimensionless numbers and other parameters are presented with a shortened label indicator with a number immediately following that indicator. The number (shown as # in the labeling key) represents the value of that dimensionless number or parameter that it is attached to. The type of mesh used for a particular simulation is indicated by a letter. These letters correspond to different mesh types as indicated in Table 5. If a specific characteristic of the simulation is different from the base model, the file name will indicate it. For example, if the simulation has a symmetry plane boundary condition at its axis as opposed to an axis boundary condition, it will be indicated in the file name. Also, these changes will be explained in the file description below it in this document. Groups of similar simulations are grouped together within common folders for organization, and several files are accompanied by a .sim file, which is not required to open the .sim file, but is useful to have.

Labeling Key:

Table 4. Labeling key for Star-CCM+ file names.

| **Parameter** | Weber Number | Reynolds Number | Ohnesorge Number | Ratio of Droplet Density to Flow's Density | Time Step | VOF Sharpening Factor | Droplet's Natural Frequency | Mesh Indication Letter |
|---|---|---|---|---|---|---|---|---|
| **Label Indicator** | We# | Re# | Oh# | RhodRhoc# | Tstep# | SF# | Tnf# | A, B, C, etc. |

For the periodic flow files, the file name will contain a label indicator for the ratio between the velocity's variation frequency and the droplet's natural frequency, fvfNF#, where # is the value of this ratio.

Example File Label:

We12_Re5000_Oh0.000865_RhodRhoc842.43_Tstep1E-4_SF0.25_Tnf0.1560_A

This file contains a simulation with a Weber Number of 12, a Reynolds Number of 5000, an Ohnesorge Number of 0.000865, a ratio of droplet density to flow density of 842.43, a Time Step of 0.0001s, a VOF Sharpening Factor of 0.25, a droplet natural frequency of 0.1560, and mesh type that is like that of type A in Table 5.

Mesh Types:

Throughout this project, different meshes were used to try and capture specific aspects of the droplet deformation, or to satisfy certain criteria such as Courant Number. The densities of each of these meshes are approximately the same for the most refined areas of the solution domains. These different meshes are indicated in the following table by different letters, which are used in the file labeling explained above.

Table 5. Mesh types with corresponding indication letters used for labeling.

| Mesh Type and Indication Letter | Mesh Description | Sample Picture |
|---|---|---|
| A | A well-defined small frustum that contains the droplet and where it deforms to during bag breakup. This model is specifically for bag breakup models. The imported CAD was 1/8$^{th}$ of a cylinder. | 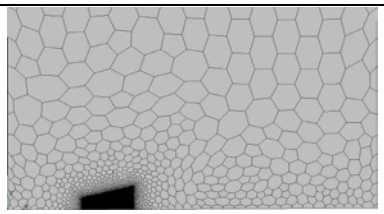 |
| B | A well-defined hemisphere to provide good initial droplet refinement. A larger frustum of less-defined mesh around and behind hemisphere. The imported CAD was 1/8$^{th}$ of a cylinder with a flat surface cut out of the wedge's point. | 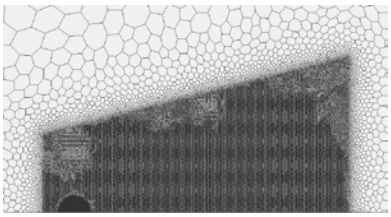 |

| | | |
|---|---|---|
| C | A well-defined hemisphere to provide good initial droplet refinement. A larger frustum of less-defined mesh around and behind hemisphere. The imported CAD was 1/8$^{th}$ of a cylinder. Has the same mesh properties as type B. | 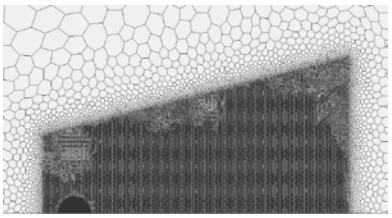 |
| D | A portion of well-defined hemisphere in bottom left to provide good initial droplet refinement. Stepped region of less-defined mesh around and behind hemisphere. The imported CAD was 1/8$^{th}$ of a cylinder. | 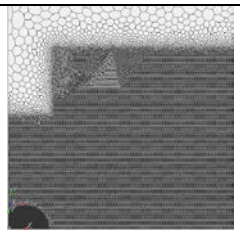 |
| E | One of the initial mesh designs. Used three different regions of varying mesh definition in area where droplet deforms. The imported CAD was 1/4$^{th}$ of a cylinder. | 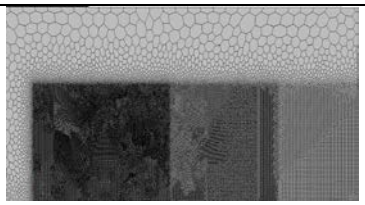 |
| F | This is the type of mesh used by Ms. Gallo in her simulations. A well-defined hemisphere is located around the droplet's initial condition. The rest of the solution domain is much less defined [2]. The imported CAD was 1/4$^{th}$ of a cylinder. | 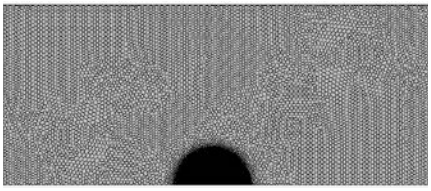 |

## 5.2 - Simulations of Drop in Zero Flow

- We0_Re0_Oh0.00109_RhodRhoc842.43_Tstep1E-3_SF0.0_Tnf0.07708_D_SymPlane

This model was developed to try and minimize the size of the solution domain, in hopes of reducing the amount of time it takes to develop the mesh, and for the simulation to run. Even though this is a zero flow case, the droplet moved, which is physically impossible. Also, the droplet oscillated far too much, which is most likely due to the imperfections of the droplet's surface, which should be smooth and spherical in an ideal setting. The program gave the error that reversed flow was occurring at a number of outlet faces, which is an error that does not effect the simulation results, but should be minimized if possible [8]. This model had the bottom surface of the solution domain defined as a symmetry plane.

- We0_Re0_Oh0.00109_RhodRhoc842.43_Tstep1E-3_SF0.0_Tnf0.07708_D_Incompress_SymPlane

This model was the same as the previous one, except that the Ideal Gas model under the Gas Eulerian Phase in the physics models was set to be incompressible (changed in the Star-CCM+ property box at the bottom of the simulation window). This was done in attempts to eliminate the droplet from moving, however it did not, and the results remained the same as those from the previous simulation.

- We0_Re0_Oh0.00109_RhodRhoc842.43_Tstep1E-3_SF0.5_Tnf0.07708_D_Incompress_SymPlane

This model tried changing the VOF Sharpening Factor to 0.5 to stop the droplet from moving and the oscillation of the droplet's surface. However, this change did not have an effect on the simulation's results.

- We0_Re0_Oh0.00109_RhodRhoc842.43_Tstep1E-3_SF1.0_Tnf0.07708_D_Incompress_SymPlane

Similar to the previous test, this model tried changing the VOF Sharpening Factor to 1.0 to stop the droplet from moving and the oscillation of the droplet's surface. However, this change did not have an effect on the results of the simulation.

- We0_Re0_Oh0.00109_RhodRhoc842.43_Tstep1E3_
  SF1.0_Tnf0.07708_D_Incompress_SymPlane_NoWall

This model used the same properties as the previous test, but set the top surface of the solution domain to be a symmetry plane instead of a wall, in hopes of decreasing any effects from a boundary layer developing over the wall. However, this change did not have an effect on the results of the simulation.

- We0_Re0_Oh0.00109_RhodRhoc842.43_Tstep1E3_

  SF1.0_Tnf0.07708_D_Incompress_SymPlane_NoYOffset

Star-CCM+ requires the user to input some offset from the y-axis for the solution domain when the axisymmetric physics condition is used. This can have some implications for the simulation in that it creates a small cylinder through the middle of the droplet, which can allow surface tension forces to effect how the droplet deforms. The solution domain was set with no offset from the x-axis, however the program would not even run without the offset.

- We0_Re0_Oh0.00109_RhodRhoc842.43_Tstep1E3_

  SF1.0_Tnf0.07708_D_Incompress_SymPlane_2D

Instead of using the axisymmetric physics model, the Two Dimensional model was used. The droplet did not move on its own as much, but the droplet still oscillated far too much for a zero flow case.

- We0_Re0_Oh0.00109_RhodRhoc842.43_Tstep1E-3_SF0.25_Tnf0.07708_C_Incompress_SymPlane

This model used the same conditions as the first test case, but it used a VOF Sharpening Factor of 0.25 and a different mesh, which was mesh type C. It was determined that there was no real difference between results for models with a VOF Sharpening Factor of 0.5 and 1.0. However, there was some noticeable difference between a factor of 0.0 and 0.5. A factor of 0.25 was chosen as a suitable value based on further testing. This mesh type was developed in order to eliminate any effects of the inlet on the droplet, and the amount of reversed flow on the outlet. This new mesh did eliminate the droplet from moving, however the droplet oscillated far too much and portions of the droplet broke off from the main mass of fluid.

- We0_Re0_Oh0.00109_RhodRhoc842.43_Tstep1E3_

  SF0.25_Tnf0.07708_C_Incompress_SymPlane_DynVisc0.088

This model tested increasing the dynamic viscosity of the droplet to 0.088 Pa-s to see if it would have a dampening effect on the surface oscillations, which it did. The oscillations were decreased by a very large amount.

- We0_Re0_Oh0.00109_RhodRhoc842.43_Tstep1E-3_SF0.25_Tnf0.07708_B_DynVisc0.088

An error was noticed in these models, which is the use of a symmetry plane boundary condition as opposed to an axis boundary condition for the solution domain's bottom surface. This error is explained more in-depth in the description of the model in which this error was first noticed, which is in section 5. 3 - Simulations of Drop in Steady Flow. A new model was developed with a CAD that had a flat portion at the location of the intended axis, which was set as an axis boundary condition in the model. An increased dynamic viscosity for the droplet was used again to minimize the amount of fluctuation of the drop's surface. Also, the incompressible node was deselected in the Ideal Gas physics model. Once again, the results showed that the movement of the droplet had been eliminated and the fluctuations of the drop's surface were minimized.

- We0_Re0_Oh0.00109_RhodRhoc842.43_Tstep1E-4_SF0.25_Tnf0.07708_B

To test the dependence of the surface fluctuations on physical conditions versus numerical conditions, the time step was decreased to 1E-4s. The results of this test were compared to the results of the test with the increased dynamic viscosity to provide an indication of which conditions had a more significant effect on the droplet's surface fluctuations. The results show that the decreased time step did decrease the magnitude of the fluctuations, but they were still more frequent and pronounced than the results with the increased dynamic viscosity. The results of this comparison are why future simulations have an increased dynamic viscosity, whenever possible.

## 5.3 - Simulations of Drop in Steady Flow

- We12_Re5000_Oh0.000731_RhodRhoc842.43_Tstep1E3_

  SF0.5_Tnf0.2579_E_Incompress_SymPlane

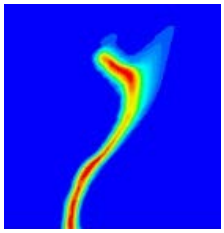

Figure 17.

This was one of the first attempts at modeling bag breakup in steady flow. The results of this simulation are interesting in that they look like a combination of both bag and shear breakup, as shown in Figure 17. The droplet initially flattens and the edge extends outward, which is similar to what has been seen in experiments. What is different from experimental results is that the edge of the droplet begins to bend downstream as if it were undergoing shear breakup, but then a portion of the droplet blows backward as in bag breakup. In normal bag breakup, the portion of the droplet along the axis of the drop blows backward, instead of near the outer edge of the flattened droplet.

- We12_Re5000_Oh0.000731_RhodRhoc842.43_Tstep1E-4_SF0.25_Tnf0.2579_E_Incompress

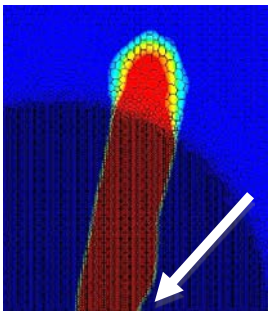

Figure 18.

At this point in the project, an error was noticed in the previous models, which was that the solution domain's bottom surface was modeled as a symmetry plane instead of as an axis. The distinction between these two boundary conditions is that a "symmetry plane" is used to indicate a plane around which the simulation is the exact same on both sides and an "axis" is used to represent the axis of a two-dimensional axisymmetric region, which is exactly what is needed for these tests. Unfortunately, this error was found after a good portion of steady flow and periodic simulations had already been run. The previous model was updated to have an axis boundary condition instead of a symmetry plane condition. The results are more like a typical bag breakup except that there is a strange pinching at the droplet's axis that develops, which is unrealistic. This pinch is indicated in Figure 18 by

the arrow. A similar model was run with a VOF Sharpening Factor of 0.5 and a larger Time Step, but the pinch formed in that simulation as well. It was hypothesized that this irregularity was due to a y-axis offset that was too large, so a new model was made with the axis projected to the x-axis. It is possible to project a boundary with an axis boundary condition to the x-axis by right-clicking on that boundary and selecting "Project to Axis…" The results of this test are unknown at this point in time.

- We12_Re6564_Oh0.0087_RhodRhoc842.43_Tstep2.42E-5_SF0.25_Tnf0.1527_B

The reason that this model was abandoned was because of how long it took to run this simulation. The results were essentially satisfying the Courant Number criteria and there had not been any fluid formation along the axis yet, but it had taken two full days for the droplet to undergo approximately half of its deformation before breakup. Due to the time constraint of this project, this simulation had to be stopped prematurely. This type of simulation would be ideal for the supercomputer, if it were converted to a version that can be run on the supercomputer.

- We11.8_Re6518_Oh0.0087_RhodRhoc842.43_Tstep5E-4_SF0.0_Tnf0.1527_B

This simulation is actually the precursor to the pervious file and is essentially the same, except that it had a larger time step. The Courant Number criteria was violated due to the larger time step, however the results of this simulation matched experimental results for bag breakup the closest. The droplet flattened and then the outer rim grew as more fluid moved outward from the center of the droplet. The center portion of the droplet then became thin and blew downstream. However, these results came on a mesh that was not very well-defined, as seen in Figure 19. Due to the positive results of this simulation, these exact characteristics were replicated in a different model with a more refined mesh (mesh type A).

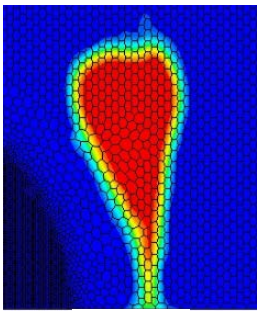

Figure 19

- We19.7_Re8414_Oh0.00087_RhodRhoc842.43_Tstep1E-5_SF0.25_Tnf0.1527_B

A smaller time step was used in this simulation to satisfy the Courant Number criteria, but it caused the simulation to take too long. Because of this, the simulation was cut short, and no meaningful results were taken from it.

- We12_Re6518_Oh0.0088_RhodRhoc842.43_Tstep2.4E-5_SF0.25_Tnf0.1527_A

This model was setup to specifically look at bag breakup, which is why the mesh contains a smaller region of well-defined mesh. This small region is intended to help minimize the amount of computational memory needed to run these simulations by minimizing the amount of small mesh cells. This mesh was also developed to help satisfy the criteria of having a Courant Number less than five. The previous tests on mesh types other than type A did not satisfy the Courant Number criteria, which raises questions about the validity of their results. Regardless, this simulation did not run until breakup because of an issue that has become a recurring problem in most of these simulations. The left image in Figure 20 shows a small amount of fluid that has developed, and travels towards the deforming droplet. This amount of fluid is produced out of nothing, which is impossible, and then impacts the droplet and produces the pinch on the right side of the droplet, as shown by the right image in Figure 20. This issue has shown up in other simulations where there is a well-defined mesh that is much larger than the droplet. In meshes such as the one used by Gallo, which have refined areas close to the initial droplet shape and then much larger cells around it, there is no evidence of this phenomena occurring. It is important to note that a large VOF Sharpening Factor can produce non-physical results such as producing fluid out of cells with no fluid in them [8]. However, tests with varying VOF Sharpening Factor values have shown that the formation of fluid out of nothing occurs for varying sharpening factor values. Also, Gallo's models used a sharpening factor of 0.5 and did not see any fluid generation, so this parameter is most likely not the only issue. The problem may be related to large areas of well-defined mesh in the solution domain and the VOF Sharpening Factor. One possible topic to

explore in the future is to produce an overset mesh, which would follow the droplet surface as it deforms, and would reduce the amount of refined mesh cells away from the droplet. This may reduce the chances of fluid generating and affecting the droplet breakup process.

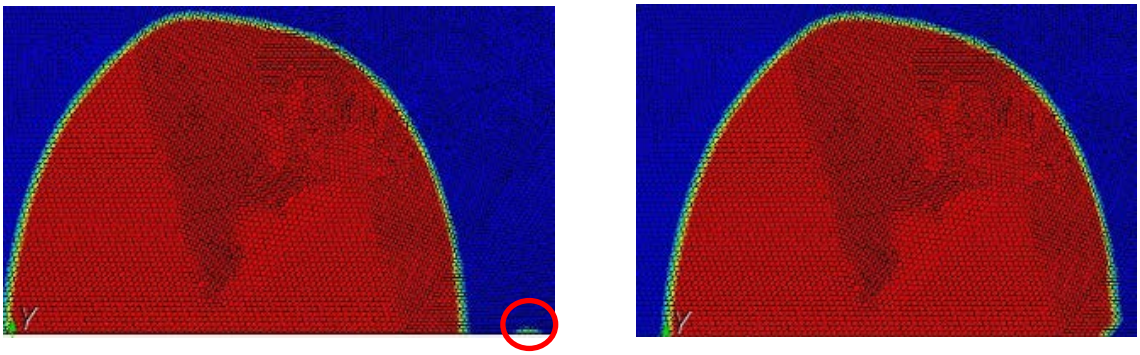

Figure 20. Example of fluid generation and impact on droplet breakup process.

- We19.7_Re900_Oh0.010_RhodRhoc842.43_Tstep2.0E-4_SF0.25_Tnf1.4274_A

The difference between this simulation and the previous one is that the time step was increased to try and make the simulation run as quickly as possible. However, t* was still large, which made the droplet take much longer to breakup than in previous simulations. As explained earlier, t* is an important factor in determining how quickly a droplet breaks up or deforms, and the smaller it is, the less time it will take for the droplet to breakup. As with the previous simulation, a mass of fluid developed along the axis that impacted the droplet and altered how it deformed.

- We25_Re638_Oh0.056_RhodRhoc842.43_Tstep2.0E-4_SF0.05_Tnf1.1398_A

A smaller VOF Sharpening Factor was used to try and minimize the formation of fluid outside of the droplet. However, this did not work and a significant amount of fluid was generated that affected the droplet deformation process. This simulation looked at a case with a Weber Number that is approximately in the middle of the Weber Number range for bag breakup

[1]. This was to ensure that the type of droplet breakup was bag breakup, and not some other regime.

- We20_Re2553_Oh0.029_RhodRhoc842.43_Tstep4.4E-5_SF0.05_Tnf0.2549_A

The droplet deformation in this test was similar to that seen in Figure 17. However a mass of fluid formed that traveled along the axis and separated the droplet from its center. The good thing about this simulation is that it satisfied, or most nearly satisfied the criteria of having a Courant Number less than five. This model was developed specifically to minimize t* as much as possible to make breakup occur quicker. The three previous simulations took very long times to complete due to large t* values.

## 5.4 - Simulations of Drop in Periodic Flow

These models analyze different ratio values of flow variation frequency to droplet natural frequency. These models do not satisfy the Courant Number criteria, and some of these models do not employ the axisymmetric physics model. Due to the periodic velocity function, Weber Number and Reynolds Number change throughout the simulation. The values for Weber Number and Reynolds Number in the file name are those for the mean flow velocity. The maximum and minimum values for Weber Number and Reynolds Number for each simulation type are presented in Table 6. These values are not specifically chosen, and a methodology is not in place for deciding what values these should be during the simulations. Most likely, these ranges will be chosen to match those in experimental results from *Secondary Droplet Breakup in Periodic Aerodynamic Flows*.

Table 6. Minimum and maximum values for We and Re in different periodic models.

| File Type | We min | We max | Re min | Re max | Breakup Regime of mean We |
|---|---|---|---|---|---|
| **We12_Re5000** | 1.4 | 32.8 | 1730 | 8270 | Bag |
| **We110_Re5000** | 100 | 120 | 15830 | 14450 | Shear |
| **We1_Re5000** | 0.5 | 1.5 | 1070 | 1820 | Vibrational |

- fvfNF0.5_We12_Re5000_Oh0.000731_RhodRhoc842.43_

  Tstep1E-5_SF0.0_Tnf0.2579_E_Incompress_SymPlane_2D

This simulation utilized two dimensional physics engine instead of the axisymmetric model. The results were similar to the deformation seen in Figure 17, except that there was a more definitive bag formation that blew downstream in this simulation. The frequency of the velocity did not appear to have much of an impact on the breakup process, which is what was hypothesized for conditions where the flow's frequency was less than the droplet frequency [1].

- fvfNF0.5_We12_Re5000_Oh0.000731_RhodRhoc842.43_Tstep2.5E4_

  SF0.5_Tnf0.2579_E_Incompress_SymPlane

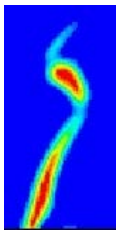

Figure 21

The only difference between this model and the previous one is that it used the axisymmetric physics engine instead of the two dimensional engine. The results are different in that there was not as much of a bag formation as there was a separation of the outer rim from the rest of the flattened droplet. A small amount of fluid developed along the axis, which caused a pinch along the axis of the droplet, similar to the one seen in Figure 20.

- fvfNF0.5_We110_Re15138_Oh0.000731_RhodRhoc842.43_Tstep2.5E4_

  SF0.5_Tnf0.2579_E_Incompress_SymPlane

At this Weber Number, the breakup should be within the shear regime, which is visualized in Table #. The results of this simulation are much different than a shear breakup, but it is difficult

to say how the droplet would have actually deformed because an amount of fluid formed along the axis and then severed the droplet through its axis. The outer edge of the droplet does exhibit some shearing effects, but it is impossible to take these results as anything meaningful due to the problem with the axis.

- fvfNF1.0_We12_Re1443_Oh0.000731_RhodRhoc842.43_Tstep2.5E4_ SF0.0_Tnf0.2579_E_Incompress_SymPlane

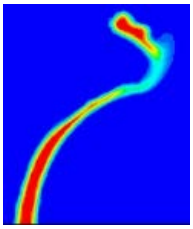
Figure 22

At a frequency ratio of one, it is hypothesized that there will be a complex droplet response [1]. The results are similar to a combination of those seen in Figure 17 and Figure 21. The outer edge of the droplet is pulled outward and then it separates from the rest of the flattened drop with a thin necked region between them. This thin region bends downstream like a shear breakup and then a portion of it blows out like in a bag breakup. There is no evidence of fluid forming along the axis and altering the breakup before the initial deformation completes.

- fvfNF5.0_We12_Re1443_Oh0.000731_RhodRhoc842.43_Tstep2.5E4_ SF0.0_Tnf0.2579_E_Incompress_SymPlane

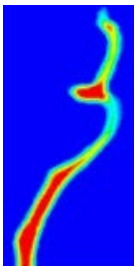
Figure 23.

For frequency ratios much higher than one, it is hypothesized that the droplet will respond to an appropriate average velocity [1]. A similar breakup process to the ones seen in Figure 17 and Figure 22 occurs in two places in this droplet. The drop's outer edge extends outward and then a portion of the fluid blows backward, as seen in the other two simulations. This exact same process seems to occur at the same time higher up on the drop. An amount of fluid generated along the axis that altered the droplet deformation, as with the other simulations.

- fvfNF5.0_We12_Re5000_Oh0.000731_RhodRhoc842.43_Tstep2.5E4_
  SF5.0_Tnf0.2579_E_Incompress_SymPlane

This model was setup to test the effect of a large VOF Sharpening Factor on the simulation of a drop breakup. The results were startling, and completely unphysical due the formation of fluid out of nothing. These results provide some insight into one possible cause of the recurring axis issue.

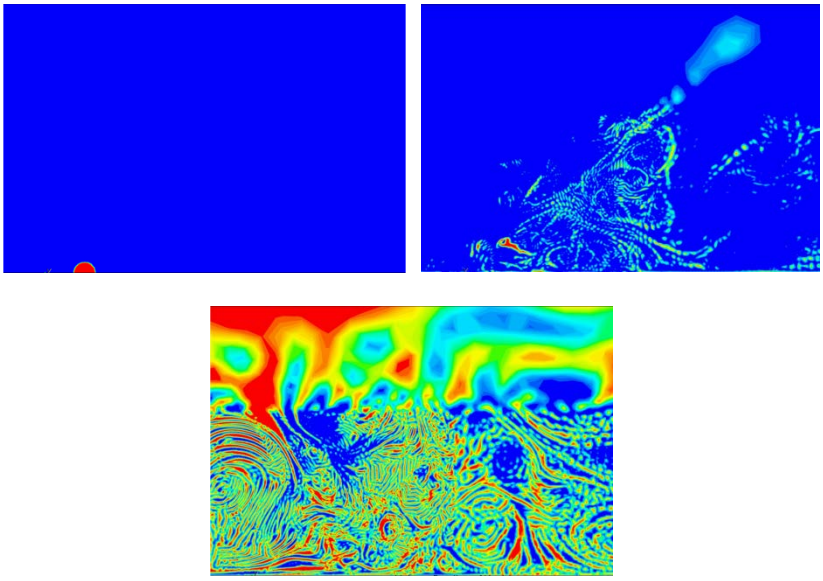

Figure 24. Example of setting the VOF Sharpening Factor too high. The middle image is approximately halfway through the simulation and the right image is the end result of the simulation.

## 6 – Discussion of Results

The primary issue with these simulations is the generation of fluid along the axis of the droplet. These generated fluid droplets move along the axis and impact the droplet, as seen in Figure 20, which alters the rest of the deformation process. It was noted that the fluid was generated for VOF Sharpening Factor values varying between 0.25 and 1.0, and that there was no generation in Gallo's simulations even though a sharpening factor of 0.5 was used. This implies that this sharpening factor is not the only element affecting this phenomenon. It was also noted

that the fluid was generated within refined mesh areas, and not in coarse mesh areas such as in Krystle's simulations. It is hypothesized that this issue is due to a combination of very small mesh cells and the VOF Sharpening Factor generating fluid within these small cells. For some mesh and sharpening factor conditions, as in Gallo's simulation, the cells are too large for the VOF model to generate any fluid. This ratio of VOF Sharpening Factor to mesh cell size at which fluid is generated is unknown, and should be explored in subsequent projects.

The results of these simulations were interesting in that they exhibited some bag-like formations for Weber Number that were within the bag breakup regime. However, the bag formations did not form along the axis of the droplet, as seen in experimental results for the same Weber Number values. Even for the simulation that best matched typical bag breakup, there was still some fluid left along the axis whereas there was none in corresponding experimental tests. This result implies that there may be more concerns with the axis of these simulations than just the generation of fluid. One possible method for eliminating any axes related issues is to model Cartesian two-dimensional droplets. One setback to this approach is that these two-dimensional simulations do not account for any three-dimensional effects that real droplets experience. These simulations are more representative of a deformable cylinder in cross flow than of a droplet in cross flow. However, there is a lot of literature available on this topic for both computational and experimental research, which would provide some comparison for these results.

An important point to make about the scope of this project is that it is specifically looking at the initial deformation of droplets, and not the entire breakup process. Once the droplet or bag portion becomes thinner than five mesh cells, the results of the simulation become questionable and are ignored after that point. Once the droplet is this thin, the model's residuals spike and increase, which makes sense due to the program trying to model an interface that is as almost as thin as a single mesh cell. An interface that is thinner than one mesh cell has a very large amount of error associated with it, and any results beyond this point are highly suspect.

The IBM Intelligent Cluster was not utilized a great deal due to issues with getting the simulations to work properly. However, it would have been a very useful tool had it been used correctly. In the near future, Union College is hiring someone to specifically work with the supercomputer and someone else who has CFD experience, which will greatly benefit students trying to use these tools for research. Hopefully these people will be able to provide specific instructions of how to use Star-CCM+ properly on the supercomputer, which will help future students acquire more results for this project. Within this project there was a difficult balance of increasing the time step as much as possible to make simulations shorter, while trying to still satisfy the Courant Number criteria. With the supercomputer capabilities, these simulations could use very small time steps to satisfy different numerical criteria without taking large amounts of time to complete. However, the biggest benefit of the supercomputer could be with meshing, which requires huge amount of computational memory, and usually take a very long time to complete. The IBM clusters would be perfect for this. Attempts were made to mesh on parallel servers for this project, but they were unsuccessful. With increased use of the IBM Intelligent Clusters, this project could make great progress.

## 7 - Future Work

The ultimate goal of this project is to illustrate the relationship between critical Weber Number and the ratio of the flow's frequency to the droplet's natural frequency. To test the hypotheses for varying ratio values presented in section 1.1 - Related Timescales of Steady and Periodic Flows, a chart will be produced that plot critical Weber Number against the ratio of the flow's frequency to the droplet's natural frequency for different ratio values, including a frequency ratio of exactly 1. This plot will help visualize the effect of a flow's frequency on the breakup process for all different ranges of frequencies. If time allows, a similar plot will be produced to visualize the effect of the flow's phase on critical We. Although these two plots will

require a large amount of simulations, the super computer will be used more frequently in future projects, which will speed up the simulation process immensely.

## 7.1 – Overset Mesh and Projection to x-axis

Before these different periodic cases can be tested, the recurring axis issue must be fixed. One possible solution for this issue may be utilizing an overset mesh. An overset mesh is one that has a larger stationary mesh within the solution domain and a smaller more-refined mesh that follows an object within the solution domain. It is possible to use this method with the VOF multiphase physics models, which is the multiphase model currently used in these models. The advantage of this method is that the stationary mesh could contain large cells, which would not generate fluid. The mesh surrounding the multiphase interface could still be refined to capture the droplet deformation, and it would follow the droplet as it deformed and moved. This would eliminate the problematic refined mesh areas downstream of the droplet's initial location.

The "Project to Axis" function was found late in this project, but this ability may have a significant effect on the simulation results. As mentioned in section 5.2 – Simulations of Drop in Zero Flow, an offset from the x-axis creates a small cylinder through the middle of the droplet, which creates large surface tension forces within the droplet. This will obviously affect the deformation process in an unrealistic way. All future simulations should employ this "Project to Axis" function to make sure that the axis of any axisymmetric simulations is actually where it should be.

## 7.2 – Two-Dimensional Droplet Breakup

As mentioned in Section 6 – Discussion of Results, another method for eliminating the axis problems is to model a whole two-dimensional ''droplet.'' This would require the development of new models and meshes, the use of different physics models, and an alteration to

the field function used to define the droplet's initial shape. Instead of using the axisymmetric model, the two-dimensional model would be used, and there would not be any axis boundaries. A proof of concept model was developed to show that it is possible to setup models of two-dimensional droplets. The results match certain aspects of the breakup found in other computational research projects very well. Sarchami, et al. provide results from a computational simulation of a two-dimensional droplet in cross flow that utilizes the Volume of Fluid method for modeling the multiphase flow. Due to the similarities between the computational models, the report from Sarchami et al. provides a great comparison for the Cartesian two-dimensional droplet model developed in this project. In Figure 25, the flow comes from the right, whereas the flow in Figure 26 comes from the left.

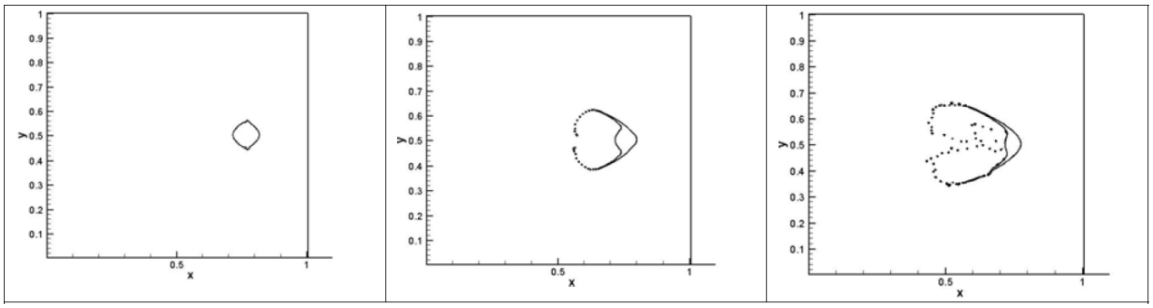

Figure 25. Sarchami et al. two-dimensional droplet breakup for We of 88 [16].

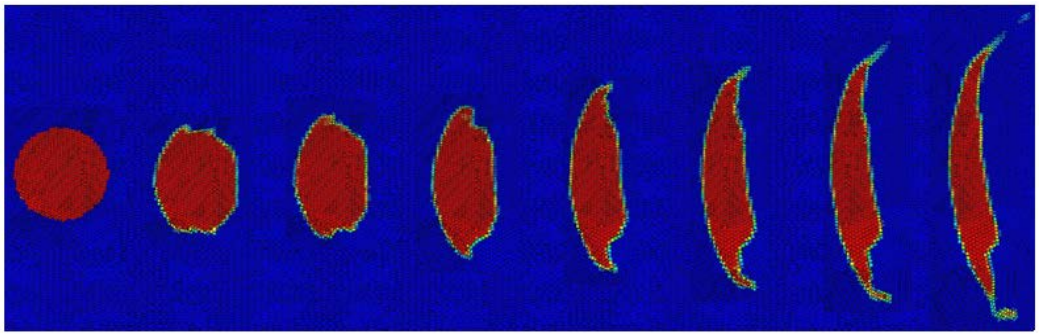

Figure 26. Droplet deformation of Cartesian two-dimensional droplet for We of 20.

The primary difference between these two models is how they model the droplet breakup after the initial deformation. The Sarchami et al. model induces vortices downstream of the droplet to produce a curling effect of the droplet's outer edges. Obviously, this present model does not do

this, and does not even consider the breakup process after the initial deformation, as explained earlier. The most likely reason for the asymmetry of the droplet deformation found in this project is due to poor mesh refinement. Without a very refined mesh to achieve a spherical initial shape, the deformation will not be perfectly symmetric. Figure 26 shows that the model from this project was able to capture the formation of pinched fluid at the top and bottom of the droplet, which is seen in the Sarchami et al. model. Although the Weber Numbers for both cases were different, the Sarchami et al. model shows that the same shearing effect of the outer edges were seen for different ranges of Weber Number. This model was not explored in detail, but these results follow what has been seen in other experiments. The Cartesian two-dimensional model should be explored more in future projects and compared to other experimental data, in order to validate a model that can then be used to model droplet breakup in periodic flows.

## 7.3 - Marble in Periodic Flow

To supplement the study of the droplet in periodic flow, an analysis of the relationship between drag coefficient ($C_D$) and Reynolds number for flows that are periodic over a solid sphere would provide more information about the different types of forces the droplet might experience in a periodic flow and how strong they might be. The relationship between $C_D$ and Reynolds Number is well understood for solid spheres in steady flows, as shown in Figure 27, but less is known for periodic flows.

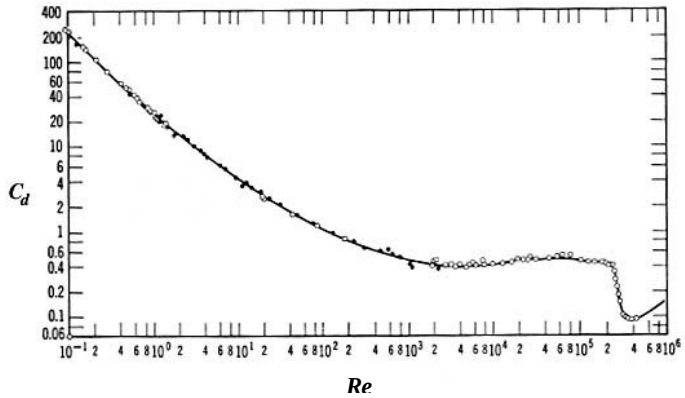


Figure 27. Drag coefficient ($C_D$) versus Reynolds number (Re) [17].

It is hypothesized that if the flow frequency is "low" enough, the $C_D$ values will match the same values from Figure 27 for the range of Reynolds Number that the flow experiences. For example, if the trough and peak Reynolds Number values for the periodic flow are 10000 and 20000, respectively, the average $C_D$ value should be close to 0.4, as shown in Figure 27. At these low frequencies, the object would be able to change velocity with the surrounding flow, and should experience conditions similar to a steady flow. The distinction between "low" and "high" frequency in this sense depends on the amount of time it takes for the flow to pass over the object, and the amount of time it takes for the flow to change. For example, at Reynolds Number of 10000 and 20000, it takes approximately 0.0021 and 0.0011 seconds, respectively, for the flow to pass over a sphere that has a 0.02 m diameter. With a frequency of 4.5 hz, the flow will undergo one oscillation in approximately 0.22 seconds. It is hypothesized that a frequency that causes the flow to oscillate one-hundred times slower than it takes for the average flow velocity to pass over the object is considered "low." Anything above this frequency would be considered "high." For this test, the velocity function should be designed to stay within the range of 10000 to 20000 because of how well the CFD model from section 4 – Marble Test Case agreed with the experimental results in this range.

Another addition to this test would be to explore Star-CCM+'s ability to model vortices behind a solid sphere profile in cross flow. It is known that vortices shed off the backend of a round object in cross flow, but the marble test case was developed to ignore this phenomenon. To improve the validity of these simulations, it must be proven that this vortices-shedding effect which occurs in nature can be modeled accurately with Star-CCM+, and then implement those capabilities into future models. This would require a profile of a full sphere, similar to the two-dimensional droplet tests.

### 7.4 - Maximum and Minimum Values of Periodic Function

The periodic functions used in this project were setup with randomly chosen maximum and minimum values. To replicate pressure waves of different intensities, research should be done to find what these maximum and minimum values are. *Secondary Droplet Breakup in Periodic Aerodynamic Flows* provides some useful information in Chapter 5 about the ranges of Weber Number for different periodic flows used in different experiments. The excel files included with the Star-CCM+ simulations provide a simple way to calculate the different inputs for the periodic function for different Weber Number and Reynolds Number ranges.

## 8 – Conclusion

This project did not complete the goal of producing accurate models of droplets in periodic flow due to a recurring issue with the axis of the droplet. However, this research effort developed and validated different components necessary for accurately modeling periodic flow conditions. Methodologies were developed to validate important numerical criteria including Courant Number and the Nyquist sampling theorem, and improvements were made over previous meshing techniques used to discretize the droplet and its deformation. A periodic velocity function was developed to accurately model a periodic pressure wave flowing passed the droplet, and it will be used in future models. Different options for correcting the axis issue were presented and discussed for future projects to tackle. Although this project did not achieve all its goals, it was an important step forward in providing insight into a fluid dynamics phenomenon that has been studied very little before.

## 9 - Bibliography


1. Bruno, Bradford A. "Secondary Droplet Breakup in Periodic Aerodynamic Flows." Thesis. Pennsylvania State University, 2000. Print.
2. "Natural Frequency and Resonance." *Natural Frequency and Resonance*. N.p., n.d. Web. 16 Oct. 2012. <http://www.cs.wright.edu/~jslater/SDTCOutreachWebsite/nat_frequency.htm>.
3. Gallo, Krystle. "Secondary Droplet Breakup in Periodic Aerodynamic Flows Using Computational Fluid Dynamics." Thesis. Union College, 2012. Print.
4. "G.M. (Gerard M.) Faeth Papers 1964-2005." *Bentley Historical Library*. University of Michigan, n.d. Web. 14 Mar. 2013.
5. Faeth, G. M. *Dynamics of Secondary Drop Breakup - A Rate Controlling Process in Dense Sprays*. Tech. Institute for Liquid Atomization and Spray Systems, 11 Sept. 2002. Web. 4 Nov. 2012. <http://www.ilasseurope.org/ICLASS/ilass2002/papers/201.pdf>.
6. Schmehl, R., G. Maier, and S. Wittig. "CFD Analysis of Fuel Atomization,Secondary Droplet Breakup and Spray Dispersion in the Premix Duct of a LPP Combustor." Proc. of Eigth International Conference on Liquid Atomization and Spray Systems, California, Pasadena. N.p., July 2000. Web. 21 Oct. 2012. <http://rschmehl.home.xs4all.nl/CV/publications/iclass2000_paper.pdf>.
7. Gallo, Krystle. "Secondary Droplet Breakup in Periodic Aerodynamic Flows Using Computational Fluid Dynamics: A Continuation of a Senior Project." Thesis. Union College, 2012. Print.
8. *User Guide STAR-CCM Version 7.04.006*. N.p.: CD-Adapco, 2012.
9. Bakker, Andre. "Applied Computational Fluid Dynamics." Lecture. Fluent Inc. Web. 4 Nov. 2012. <www.bakker.org>.
10. *Star-CCM+ Tutorial Guide*. CD-adapco, n.d. Web. 6 Nov. 2012. <file:///C:/Program%20Files/CD-adapco/STAR-CCM+7.02.008/doc/online/wwhelp/wwhimpl/js/html/wwhelp.htm#href=tutorials.307.1.html>.
11. Fox, Robert W., Alan T. McDonald, and Philip J. Pritchard. *Introduction to Fluid Mechanics*. 6th ed. New York: J. Wiley, 2004. Print.
12. Bakker, Andre. "Lecture 14 - Multiphase Flows." Fluent Inc., n.d. Web. 30 Oct. 2012. <www.bakker.org>.
13. Tryggvason, Grétar, Ruben Scardovelli, and S. Zaleski. *Direct Numerical Simulations of Gas-liquid Multiphase Flows*. Cambridge: Cambridge UP, 2011. Print.
14. Hirt, C. W., and B. D. Nichols. "Volume of Fluid (VOF) Method for the Dynamics of Free Boundaries." *Journal of Computational Physics* 39 (1981): 201-25. Web. 31 Oct. 2012. <http://pages.csam.montclair.edu/~yecko/icodes/HirtNichols_Surfer_JCP1981.pdf>.
15. Dimensionless Numbers and Courant Number, Microsoft Excel
16. Sarchami, Araz, Ali Jafari, and Nasser Ashgriz. *Breakup of a 2D Drop in Cross Flow*. Tech. N.p.: n.p., n.d. Print."Drag Coefficients." *Project Links*. N.p., n.d. Web. 06 Nov. 2012. <http://www.ibiblio.org/links/devmodules/dragforces/html/fluids_link.html>.